Elastic properties of a reservoir sandstone: a broadband inter-laboratory benchmarking exercise

Abdulwaheed Ògúnsàmì, Ian Jackson, Jan V.M. Borgomano, Jérôme Fortin, Hasan Sidi, Andre Gerhardt, Boris Gurevich, Vassili Mikhaltsevitch, Maxim Lebedev

Elastic properties of a reservoir sandstone: a broadband inter-laboratory benchmarking exercise

Abdulwaheed Ògúnsàmì[1], Ian Jackson[1], Jan V.M. Borgomano[2], Jérôme Fortin[2], Hasan Sidi[3], Andre Gerhardt[3], Boris Gurevich[4], Vassily Mikhaltsevitch[4] and Maxim Lebedev[4]

[1] Research School of Earth Sciences, Australian National University, Canberra, Australia

[2] Laboratoire de Géologie, Ecole Normale Supérieure/CNRS, UMR8538, PSL Research University, Paris, France

[3]Woodside Energy Ltd, Perth, Australia.

[4]Centre for Exploration Geophysics, Curtin University, Perth, Australia.

Corresponding author: **Abdulwaheed Ògúnsàmì** (Abdulwaheed.ogunsami@anu.edu.au)

Abstract

Low-frequency forced-oscillation methods applied to a reservoir sandstone allowed determination of the Young's modulus and Poisson's ratio (from axial loading), bulk modulus (by oscillation of the confining pressure), and shear modulus (from torsional forced-oscillation), for comparison with conventional ultrasonic data. All tests were performed on a common sandstone core sample from an oil reservoir offshore West Africa. The results show a steady increase in ultrasonic velocities and shear modulus of the dry specimen as functions of pressure, which suggests a progressive closure of the inter-granular contacts. An increase of bulk and Young's moduli and Poisson's ratio is observed on decane-saturation of the sample when tested with a sufficiently small dead volume. This observation, consistent with Gassmann's theory, suggests that such measurements probe undrained (saturated isobaric) conditions. Diminution or absence of such fluid-related stiffening for low-frequency measurements with dead volumes comparable with the pore volume of the specimen indicate partially drained conditions and highlight the critical role of experimental boundary conditions. Directly measured bulk and shear moduli are consistent with those derived from Young's modulus and Poisson's ratio. These results of the inter-laboratory testing using different measurement devices are consistent in terms of the effect of frequency and fluid saturation for the reservoir sandstone specimen. Such broad consistency illustrates the validity of forced-oscillation techniques and constitutes an important benchmarking of laboratory testing of the elastic properties of a porous medium.

1.0 Introduction

Time-lapse (4D) seismic technology is an important reservoir monitoring tool for the oil and gas industry (e.g. Capello & Batzle, 1997; Lumley & Behrens, 1998; King, 2009). The technology involves the

acquisition, processing and interpretation of repeated three-dimensional (3D) seismic surveys over a producing field in order to understand production-related changes and their impact on the elastic properties of the reservoir. The success of such technology depends partially on the sensitivity of measured seismic attributes (such as acoustic impedance and V_P to V_S ratio) to changes in reservoir conditions such as effective pressure and fluid saturation (e.g. Lumley et al., 1997; Wang, 1997). The sensitivity can be established by laboratory testing of the elastic properties of core samples as a function of effective pressure and fluid saturation.

Conventionally, laboratory testing is done using the ultrasonic wave-propagation techniques (Gregory & Podio, 1970; Birch,1960; Han et al.,1987).At ultrasonic (MHz) frequencies, however, the pressure dependence of elastic moduli of fluid saturated rocks may be much weaker than at seismic frequencies due velocity dispersion (Mavko & Jizba, 1991;Gurevich et al., 2010; Müller et al., 2010). In dry granular rocks such as sandstones, the pressure dependence of elastic moduli of the rock is primarily controlled by pressure-dependent compliance of grain-to-grain contacts, which are usually much softer than the grain mineral itself. In a fluid-saturated rock, the pore fluid may stiffen these contacts, and this stiffening is frequency-dependent. At seismic frequencies, there is enough time in one wave period for the fluid to squeeze out of the contact area into the larger pore space, and hence the contacts are almost as compliant as in the dry rock. Conversely, at ultrasonic frequencies, the wave period is insufficient for the fluid to squeeze out, so that the fluid is effectively trapped in the contact area, reducing the compliance of the contact to almost zero. Thus, the ultrasonic moduli of a fluid-saturated rock are often much less sensitive to confining or fluid pressure than the moduli measured at seismic frequencies. This effect, known as squirt flow dispersion (e.g. Mavko & Nur, 1975; O'Connell & Budiansky, 1977), is one of the reasons as to why ultrasonic measurements on fluid-saturated samples are often inadequate for calibration of seismic measurements.

Due to strong velocity dispersion in fluid saturated rocks, time-lapse seismic feasibility studies (e.g. MacBeth, 2004; Holt et al., 2005; Asaka et al., 2018) commonly assess the sensitivity of elastic properties to pressure and saturation using measurements on dry cores combined with the Gassmann theory. However, the process of drying reservoir samples may potentially modify the property of the rock matrix and introduce additional complications.

Forced-oscillation technique of the 'stress-strain type' (Spencer, 1981; Batzle et al., 2006) constitutes a promising alternative approach. The technique provides for the measurement of the elastic properties of rocks under low-frequency, low strain loading conditions that broadly simulate those of typical porous reservoirs. In recent decades, there have been several laboratory investigations using the forced-oscillation technique (e.g. Adam et al., 2006; Adam et al.,2009; Adelinet et al., 2010; Li et al., 2014; Pimienta et al. 2015, Mikhaltsevitch et al., 2014). However, the technique is relatively new, rapidly developing, and further studies are required to validate its reliability (see overview in Subramaniyan et al.,2014). Furthermore, different studies use different measurement systems or tested different reservoir rocks. To the best of our knowledge, no effort has been made to cross-validate the various results.

The study presented in this paper fills this gap. For a single cylindrical core specimen, we performed a systematic inter-laboratory testing of elastic properties of a porous reservoir sandstone using three different forced-oscillation measurement devices. The specimen was tested both in dry and decane-saturated conditions to document the fluid-saturated and pressure-dependent elastic properties of the reservoir specimen. Results from the different measurement devices were compared and interpreted using rock physics theories. Our findings demonstrate the consistency of the results between the three measurement devices within a reasonable measurement error.

2.0 Methods

2.1 Specimen

The test specimen is a homogenous reservoir sandstone sampled from a depth of 2660 m from an oil field offshore from NW Africa. Petrographic and XRD analyses of rocks from the relevant depth interval within this formation indicate moderately well sorted but poorly compacted sandstone comprising 60.5-70% detrital minerals (mainly quartz), 18.5-29.5% diagenetic infill (mainly the carbonates dawsonite, calcite and dolomite), and 4.5-12% clay. We obtained a cylindrical core-plug specimen - initially 79.5 mm in length and 38.5 mm in diameter - for tests at Curtin University and the École Normale Supérieure (ENS). Later this sample was re-cored to a smaller dimension (75 mm in length and 15 mm in diameter) for testing at the Australian National University (ANU). The porosity and permeability estimated from petrophysical logs are ~ 30% and 120 mD (1.2 ×10-13 m2), respectively. To study the fabric and crack-related microstructure, we obtained X-ray tomographic images of the specimen at ambient conditions. To evaluate the possible matrix damage and extent of microstructural changes during the test possibly due to the drying, we measured the porosity from the weight of the dry and fully saturated specimen (as 29%) following completion of the first phase of the experimental work at Curtin University.

Test specimen			
Porosity, $\boldsymbol{\Phi}$	Permeability (mD)	Density (kg/m^3)	K_{matrix}(GPa)
29%	120	1933.2	33.1
n-Decane pore fluid			
Temp. (^{o}C)	Viscosity (Pa.s)	Density (kg/m^3)	K_f (GPa)
20	9.68×10^{-4}	734.2	1.21

Table 1: Physical properties of the test specimen and the pore fluid. K_{matrix} is the bulk modulus for the mineral skeleton required to reconcile the observed fluid-related stiffening of the bulk modulus with the Gassmann model**.** K_f is the fluid bulk modulus.

The elastic properties were measured both in dry and fully-saturated conditions with n-decane, a well-characterised liquid hydrocarbon. Table 1 summarises the physical properties of the specimen as well as the physical properties of the n-decane pore fluid, obtained from the webbook of the National Institute of Standards and Technology (NIST).

2.2 Experimental Set-up

We used three complementary forced-oscillation techniques in different rock physics laboratories: Axial stress oscillation both at Curtin and ENS, confining pressure oscillation at ENS, and torsional oscillation at the ANU. We also measured the elastic properties of the specimen using the ultrasonic wave propagation method both at Curtin and ENS.

2.2.1 Oscillation of axial stress and confining pressure – Young's modulus, Poisson's ratio, and bulk modulus

We measured Young's modulus and associated dissipation, along with Poisson's ratio of the reservoir sandstone specimen with the low-frequency axial stress oscillation apparatus (Figure 1) both at the Curtin University and ENS (Borgomano et al., 2017; Mikhaltsevitch et al., 2014). The working principle for the set up at both laboratories is similar except that the apparatus at ENS has additional capacity for measurements involving oscillation of the hydrostatic pressure – allowing the direct measurement of the bulk modulus. The confining medium for each apparatus is hydraulic oil. Pore pressure within the cylindrical test specimen, for each set-up, can be independently applied and controlled. By applying a sinusoidally time-varying axial stress or confining-pressure perturbation to the rock, we estimate the dynamic moduli (Young's and bulk), Poisson's ratio and associated dissipation by measuring the resulting

axial and circumferential strains on the rock sample and the axial strain in the reference aluminium material (Borgomano et al., 2017; Mikhaltsevitch et al., 2014). The essential parts are a force generator, a force sensor to measure the applied stress and a displacement sensor to measure the resulting strain. In both set-ups, aluminium cylinders 38.5 mm in diameter constitute the end platens which serve as the elastic reference. A piezoelectric actuator, mounted between the axial piston of the cell and the top end platen, is used to apply the oscillating axial force to the jacketed cylindrical specimen. For the test involving oscillation of the confining pressure (e.g. Adelinet et al., 2010; David et al., 2013; Pimienta et al., 2015), the pressure-control system is used to perturb the confining pressure, providing low-amplitude hydrostatic stress oscillation around a mean value of confining pressure. The amplitude of pressure oscillation ΔP_c, and the resulting volumetric strain, are sufficiently low that the material's response to stress is linear (Pimienta et al., 2015).

The aluminium platen, used as the reference material, is equipped with two axial (and four at ENS) strain gauges which act as the axial stress sensor (Mikhaltsevitch et al., 2014; Borgomano et al., 2017). The average of the strains ($\varepsilon_{al,av}$) obtained from these gauges is used, together with the known Young's modulus of aluminium ($E_{al,av}$ = 72GPa, Mavko et al., 2009) to obtain the axial stress, $\sigma_x = E.\ \varepsilon_{al,av}$. The axial ($\varepsilon_{ax}$) and circumferential (radial) (ε_{rad}) strains in the test specimen are obtained from the axial and circumferential strain gauges glued directly onto the specimen. This gives Young's modulus E of the specimen as the ratio of the axial stress to the specimen's axial strain. Poisson's ratio ν is obtained as the ratio of the amplitudes of the radial and axial strains,

$$E = \frac{\sigma_X}{\varepsilon_{ax}} \text{ and } \nu = -\frac{\varepsilon_{rad}}{\varepsilon_{ax}} \quad (3)$$

Furthermore, given the Poisson's ratio and Young's modulus, the bulk K_{ax} and shear G_{ax} moduli of the (isotropic) medium can be inferred as follows:

$$K_{ax} = \frac{E}{3(1-2\nu)} \text{ and } G_{ax} = \frac{E}{2(1+\nu)} \quad (4)$$

For the forced-oscillation of the confining pressure, the ratio of the hydrostatic stress to the resulting volumetric strain $\varepsilon_{vol} = \varepsilon_{ax} + 2\varepsilon_{rad}$ provides the bulk modulus K as:

$$K = -\frac{\Delta P_c}{\varepsilon_{vol}} \quad (5)$$

We then obtained the associated dissipation Q^{-1} from the phase difference $\Delta\phi$ between the applied stress ϕ_{stress} and resulting strain ϕ_{strain} (i.e. $\Delta\phi = \phi_{stress} - \phi_{strain}$). The Young's dissipation is obtained from the phase shift between the axial stress σ_{ax} and axial strain ε_{ax}, $Q_E^{-1} = \tan(\phi\sigma_{ax} - \phi\varepsilon_{ax})$. The bulk dissipation ($Q_K^{-1}$) for the hydrostatic oscillation is obtained from the phase shift between the hydrostatic stress ΔP_c and the volumetric strain ε_{vol}, as $Q_K^{-1} = \tan(\phi_{\Delta Pc} - \phi\varepsilon_{vol})$.

At ENS, the specimen was tested for different amounts of so-called dead volume. The dead volume (i.e. the volume of fluid in the reservoir drainage system or pipelines connected to the ends of the sample) has an important implication on the interpretation of drainage regime of laboratory tests and must be carefully considered (Pimienta et al., 2016; Mikhaltsevitch et al., 2019). Indeed, the apparent elastic modulus of the sample will depend on the dead volume for frequencies below the drained/undrained transition. Thus, the valves, which control the dead volume, were kept open for adjustment of confining and pore pressures but are closed during forced-oscillation measurements.

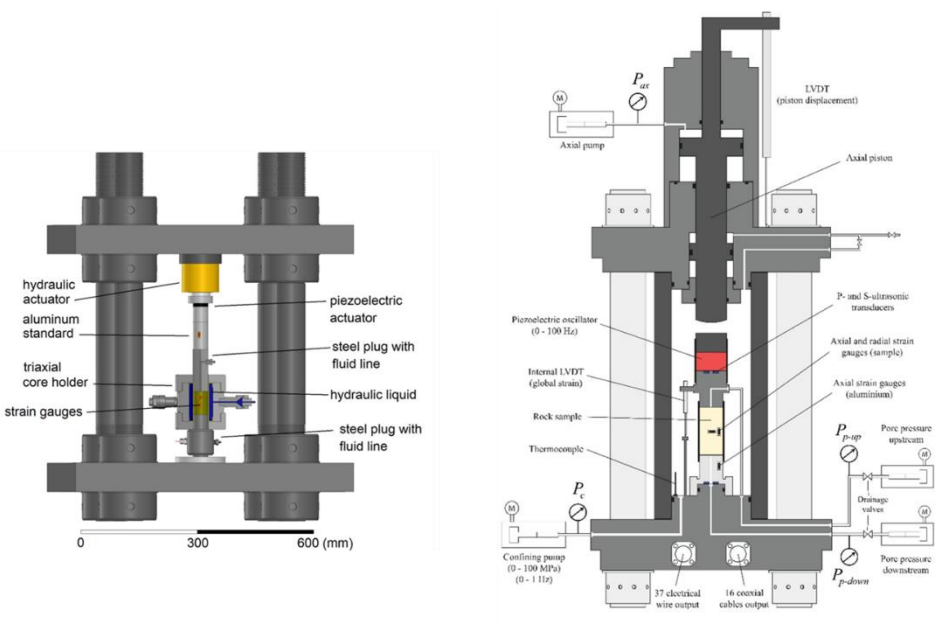

Figure 1: A schematic of the low-frequency laboratory apparatus, on the left for Curtin University (Mikhaltsevitch et al., 2014) and on the right for ENS (Borgomano et al., 2020)

2.2.2 Torsional forced oscillations – Shear modulus

Torsional forced-oscillation tests have been conducted on the specimen in dry and saturated (n-decane) conditions using the attenuation apparatus at the Australian National University (Jackson & Paterson, 1993; Lu & Jackson, 1996). This apparatus is a gas-medium rig with capacity for high-pressure conditions (up to 200 MPa), along with independent application and control of pore fluid pressure on a cylindrical specimen of 15 mm in diameter and up to 150 mm in length. A more detailed description of the setup and relevant modifications has been recently provided elsewhere (e.g. Cline & Jackson, 2016; Li et al., 2018; Ògúnsàmì et al., 2020).

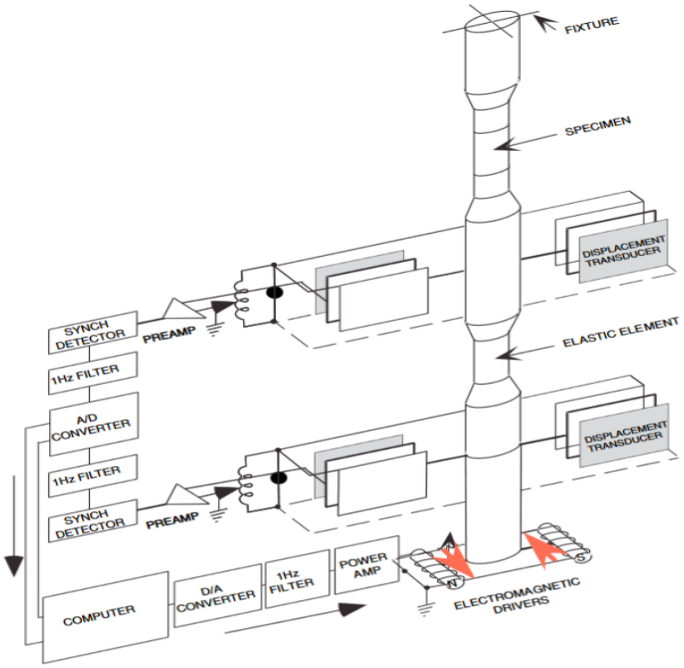

Figure 2: A schematic of the attenuation apparatus at the ANU.

We obtained the shear modulus and associated dissipation of the sandstone specimen at mHz – Hz frequencies from the analysis of the response of the composite beam of Fig. 2 to the application of an oscillating torque. The beam consists of the test specimen that is connected in series to an elastic standard of known mechanical properties. Displacements associated with the twist of the beam, upon application of torque, are measured by two pairs of three-plate capacitance transducers. The distortion of the specimen assembly, containing the specimen of interest along with steel connecting rods, relative to that of the hollow steel elastic element, provides an interim indication of the complex compliance (including the phase lag between applied torque and resulting distortion). The shear modulus and dissipation (Q_G^{-1}) for the test specimen are computed from the complex compliance differential between the specimen and reference assemblies (containing a control specimen of intact glass), along with the known shear moduli for the control specimen and enclosing annealed copper jacket (Jackson & Paterson, 1993; Lu & Jackson, 2006).

2.2.3 Ultrasonic measurements

Ultrasonic tests were performed both at Curtin University and ENS using the standard pulse transmission techniques (Birch, 1960). At Curtin University, we used an apparatus with a slightly modified set of units placed between the steel platens (Figure 3). The transducers are inserted in steel end-caps where they are fixed on the end butts facing a sample by steel springs. At ENS, the ultrasonic transducers embedded in each end platen of the axial oscillation set up described in section 2.2.1 were used for measurement of the ultrasonic velocities in conjunction with the low-frequency oscillation of axial stress or confining pressure. The central frequencies for the P- and S- wave ultrasonic transducers are 1 MHz and 0.5 MHz, respectively. The errors for the measured P-wave and S-wave velocities are less than 2% and 5%, respectively, originating from the uncertainties in sample's length and the determination of the first arrival time of P- and S- waves.

2.3 Experimental protocols

The low-frequency tests at both Curtin and ENS were first performed on a dry specimen at confining pressure P_c = 10 MPa before testing the decane-saturated specimen at 10 MPa differential pressure (P_{eff} = $P_c - P_f$). The experimental assemblies have different dead volumes: 2 cm^3 at Curtin, optionally 3.3 cm^3 or 50 cm^3 at ENS, and 42 cm^3 at ANU. Standard industry practice is to clean reservoir core specimens before any laboratory testing. Such cleaning involves the use of solvents, e.g. 50/50 mixture of toluene/methanol with 1% of ammonium hydroxide, to remove any contaminant/residue from the in-situ hydrocarbon. For this test, however, no such cleaning was performed to minimise the change of the specimen's properties. So dry conditions for the test at Curtin implies 'as received' without any desiccation or oven-drying. The specimen was only oven-dried in other laboratories, prior to testing to reduce the effect of moisture. At ENS, for example, the specimen was oven-dried for two days at 60-70°C before measurement. In both laboratories, the ultrasonic measurements were made at a 0-15 MPa range of confining pressures for the dry conditions and at a 0-15 MPa range of differential pressure for the

saturated conditions. For both ultrasonic and low-frequency test, pore fluid pressure P_f was fixed at 5 MPa.

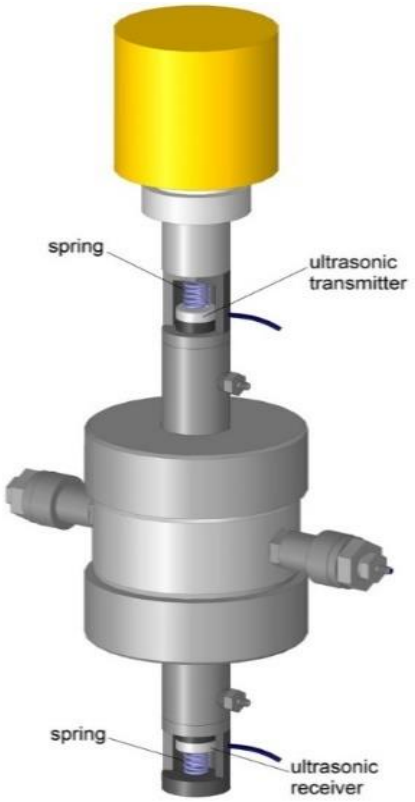

Figure 3. The arrangement for ultrasonic measurements at Curtin University (Mikhaltsevitch et al., 2014)

At the ANU, we first investigated the oven-dried specimen at a range of confining pressures before testing the decane-saturated specimen. For the saturated conditions the pore fluid pressure was held constant at 5 MPa and we varied the confining pressure to achieve differential pressures of 4 -15 MPa. We charged the pore fluid line with n-decane and the pore-fluid pressure within the specimen was allowed to equilibrate for more than 24 hours to ensure uniform pore pressure in the specimens, before testing the mechanical properties. Between successive measurements of mechanical properties at varied

differential pressures, we explored the possibility of taking permeability measurements, using the transient-flow approach, to further guarantee that the reservoir sandstone specimen was saturated correctly and that the pore pressure is in equilibrium. No permeability data, however, were successfully obtained – as we shall discuss later. Nonetheless, our saturation procedures are designed to achieve the closest possible approach to conditions of full saturation. For instance, the saturation and fluid charging procedure at ANU, involving a protocol of sustained evacuation of the entire pore fluid system and bleeding of any residual gas, is terminated upon a sudden rise of pore pressure with incremental advance of the piston within the pore-fluid intensifier - indicative of saturation of the pore space with an incompressible pore fluid. At ENS, the specimen was fully-saturated using a specific procedure described as follows; a vacuum was generated throughout the whole sample from a vacuum pump connected on the top pore line. The pore fluid is then injected from the bottom of the sample. The vacuum pump is connected to the top pore line via a transparent tube which enables us to see the fluid movement from one end of the sample to the other. Moreover, the volume injected by the fluid pumps can be monitored. Finally, a volume of fluid of at least 2–3 times the pore volume, is drained through the sample to ensure the absence of air bubbles.

3.0 Results

3.1 Young's modulus and Poisson's ratio

Measurements of Young's modulus along with the corresponding strain-energy dissipation ($\boldsymbol{Q_E^{-1}}$) and the Poisson's ratio were made on the sandstone reservoir specimen under dry and decane-saturated conditions, at 10 MPa differential pressure (P_f = 5 MPa), using axial forced-oscillation tests at Curtin University and ENS. Figure 4 shows the Young's modulus along with the corresponding strain-energy dissipation and the Poisson's ratio plotted as a function of frequency for both dry and saturated conditions.

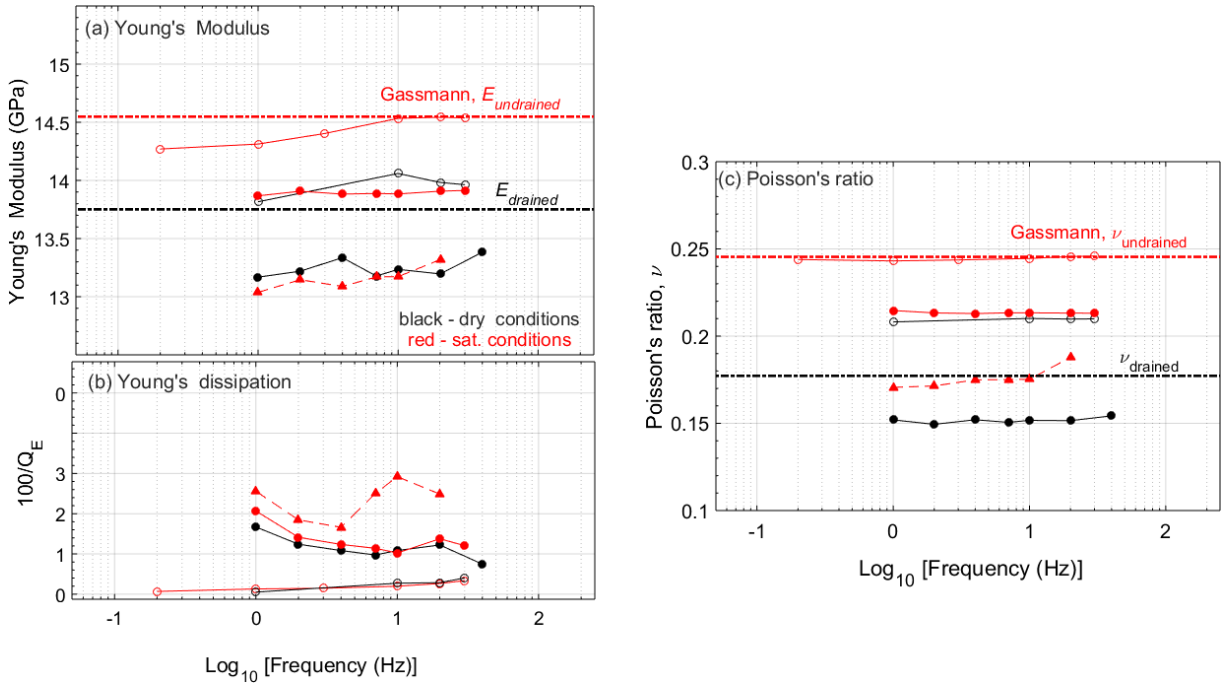

Figure 4: Frequency-dependent elastic properties (E, Q_E^{-1} and Poisson's ratio) of the reservoir specimen at dry (black symbol) and decane-saturated (red symbol) conditions assessed under axial forced-oscillation at Curtin University (open circle symbols) and ENS (filled circle symbols for small dead volume and filled triangle symbols for large dead volume). Dashed straight lines show the predictions based on Gassmann's theory. Differential pressure at 10 MPa.

A broadly similar Young's Modulus, averaging 13.5 ± 0.5 GPa, is measured for the dry conditions in both labs, without any systematic frequency dependence. In addition, for the dry specimen, the Poisson's ratio are found constant with frequency with a value of 0.17 ± 0.02.

The fluid-saturated specimen shows systematically higher values of Young's modulus than for dry conditions (except for ENS with large dead volume). The Young's modulus suggests a mild frequency dependence – most clearly with the results of the test at Curtin – tending to increase with increasing frequency. Substantial strain-energy dissipation consistently matches the observed dispersion of Young's modulus. Note that the difference between the dry and saturated Young's modulus (Curtin and small dead volume of ENS) is similar in both labs and equal ~ 0.6 ± 0.2 GPa.

The Poisson's ratio of the saturated sample is higher than for a dry sample. Thus, the results of Young's modulus and Poisson's ratio from the two independently conducted tests at both labs are broadly consistent both in terms of the fluid and frequency dependence.

3.2 Shear modulus

Using the Jackson-Paterson apparatus at the ANU, we measured the shear modulus and dissipation of the re-cored specimen – in both dry and decane-saturated conditions. With a constant pore pressure of 5 MPa, the reservoir sandstone specimen was tested at a range of differential pressure (up to 15 MPa) by varying the confining pressure. In Figure 5, we summarise the shear modulus as a function of the measurement frequency and pressure.

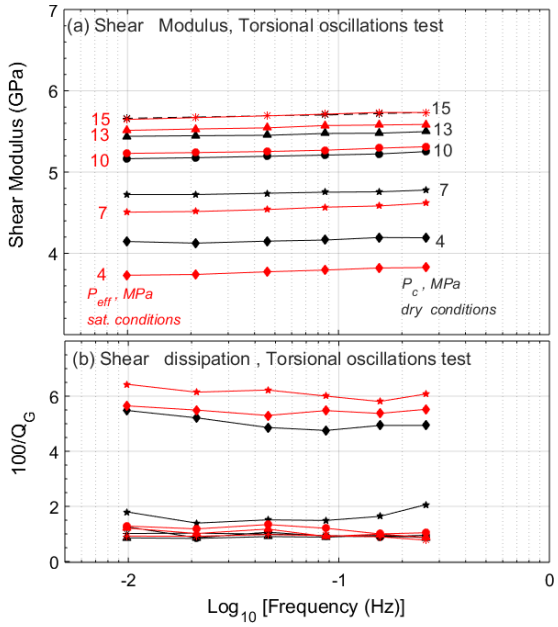

Figure 5: Shear modulus and dissipation of the dry (black symbol), and decane-saturated (red symbols) specimen measured with torsional forced-oscillations using the Jackson –Paterson apparatus at the ANU. Pore pressure fixed at 5MPa and confining pressure varied accordingly. The uncertainty associated with the determined modulus is ± 3%

The results show a systematic sensitivity of shear modulus to increasing pressure both in dry and saturated conditions. Dry shear modulus of 4.2 GPa measured at P_c = 4 MPa increases progressively to 5.6 GPa at 15 MPa.

The shear modulus for both dry and saturated specimens shows only mild dispersion across the frequency range of the test. On decane-saturation, the shear modulus of the reservoir specimen remains essentially unchanged. Subtle differences between the dry and decane-saturated shear moduli at the lowest values of confining/differential pressure may not be resolvable given the uncertainties of order 0.5 MPa in pressure.

For both dry and saturated-conditions, the shear dissipation shows no systematic frequency dependence. Pressure and fluid sensitivity of the shear dissipation is observed only for measurement at $P \leqslant 7$ MPa, where values of $\boldsymbol{Q_G^{-1}}$ range between 0.02 and 0.06. Overall, shear modulus and dissipation are concluded to be essentially frequency –independent.

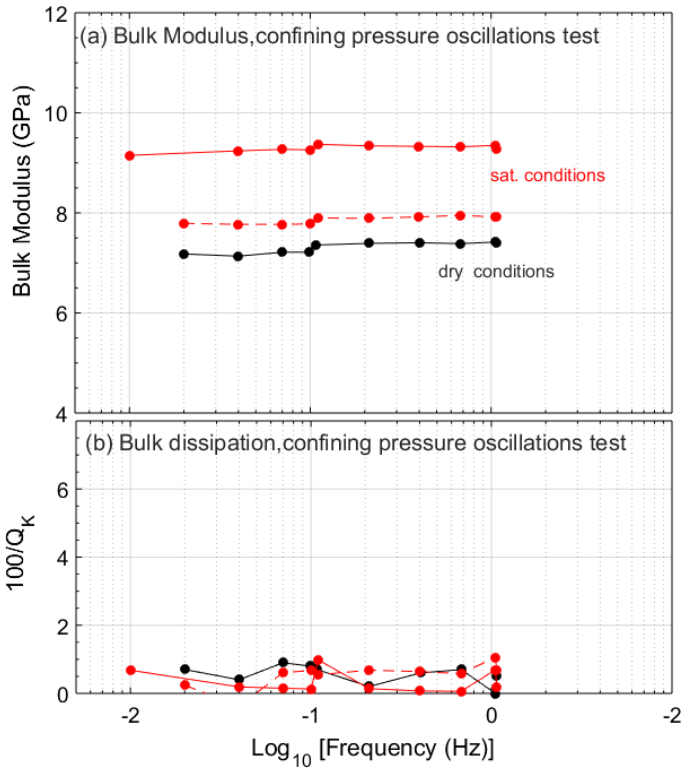

Figure 6: Bulk modulus and dissipation of the dry (black symbol) and decane-saturated specimen (red symbols, small dead volume with a solid line and large dead volume with the dashed line) measured with a test involving the oscillation of the confining pressure at ENS. Differential pressure at 10 MPa.

3.2 Bulk modulus

Figure 6 shows the results of the test involving oscillation of the confining pressure at 10 MPa differential pressure conducted at ENS as described in section 2.2.1. The figure shows the frequency dependence of the bulk modulus and dissipation for both the dry and decane-saturated conditions of the reservoir sandstone specimen.

The bulk modulus of ~7 GPa is observed for the dry conditions. The modulus and dissipation for the dry specimen are essentially frequency-independent. Upon saturation with n-decane, the bulk modulus is markedly increased by ~7 % and ~ 27 % relative to bulk modulus of the dry condition for the large and small dead volumes, respectively.

The observed dissipation Q_K^{-1} of ~ 0.01 is broadly similar for both dry and saturated-conditions. Besides, the bulk modulus and dissipation Q_K^{-1} for the decane–saturated conditions show no systematic frequency –dependence.

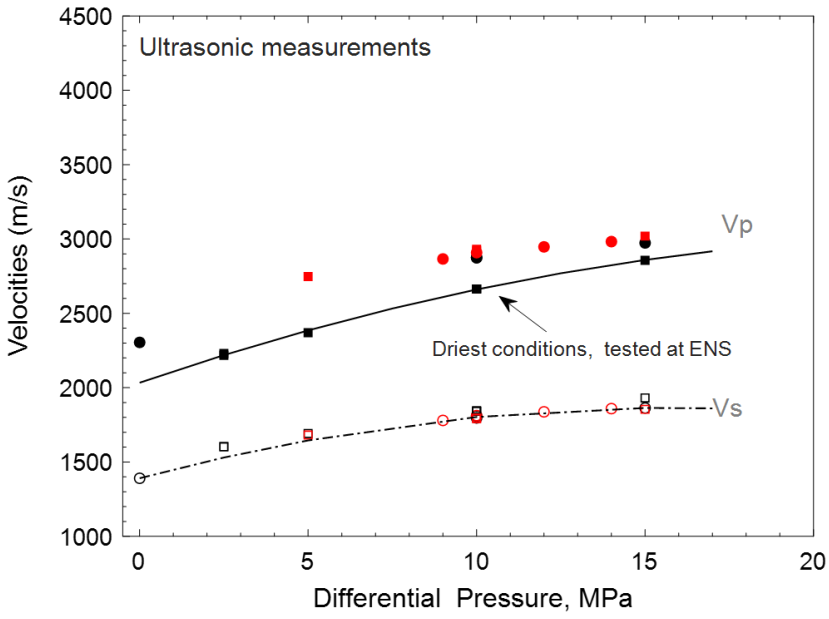

Figure 7: Pressure-dependent ultrasonic velocities of the specimen obtained by the pulse transmission techniques for the dry (in black) and decane-saturated conditions (in red symbols) both at Curtin University (denoted with circles) and ENS (denoted with square). Filled symbols for V_P, and open symbols, for V_S.

3.3 Ultrasonic measurements

To provide further information on the frequency dependence of the elastic properties beyond the frequency covered by the forced-oscillation techniques, ultrasonic measurements of the velocities were performed in both the Curtin and ENS labs using the pulse transmission technique. Here we summarise the pressure dependence of the ultrasonic velocities for dry and decane-saturated conditions (Figure 7).

With a fixed pore pressure at 5 MPa, the confining pressure was varied to enable testing at a range of differential pressure for the decane-saturated conditions.

Overall, the results obtained from both labs are broadly consistent in that they show a consistent pressure sensitivity of the velocity both in dry and saturated conditions. For example, the *P*-wave velocity at ambient (bench-top) pressure conditions of ~2300 m/s measured at Curtin for the dry specimen systematically increases to 3000 m/s at 15 MPa confining pressure – a trend consistently similar with the results for n-decane-saturated conditions, tested both at Curtin and ENS. However, the values of the *P*-wave velocities for the dry conditions, measured at both labs, are somewhat different. At P_c = 10 MPa, for example, the measured velocity for the dry conditions at ENS lab (2600 m/s) is lower than the one obtained at Curtin (2800 m/s).

Whereas the measured velocities for the decane-saturated conditions from both labs are broadly consistent, the fluid sensitivity is different – possibly because the specimen tested at ENS was oven-dried whereas the same specimen was tested 'as received' at Curtin University. Overall, the high-frequency velocity results from both tests indicate consistent, systematic pressure sensitivities for both in dry and fluid-saturated conditions, with somewhat diminished pressure sensitivity for decane pore fluid saturation.

4.0 Discussion

4.1 Dry conditions

Pressure sensitivity of elastic properties

The systematic increase in shear modulus and ultrasonic velocities with increasing pressure observed for both the dry and decane-saturated conditions is consistent with the expectation of the effect of pressure-related closure of compliant (crack-like) porosity in a porous medium (Walsh, 1965, Sayers, 2005; Fortin et al., 2005). Such compliant porosity in sandstones is primarily associated with the grain-to-grain contacts. We interpret the pressure sensitivity as related to the deformation of the compliant grain-to-grain contacts which is consistent with the weakly-cemented nature of the reservoir sandstone facies. The

implication from the theory of Walsh (1965) using $P = E\alpha$ – with dry Young's modulus E of 13.8 GPa and a closure pressure, P of 10 MPa – is that the inter-granular contacts must have an indicative aspect ratio $\alpha < 7 \times 10^{-4}$. Such inference is broadly consistent with published values of aspect ratio for sandstones (e.g. Cheng & Toksöz, 1979; Siggins & Dewhurst, 2003; Pimienta et al., 2015). Note that features with such low-aspect-ratio cannot be detected by X-ray micro-CT, which has a matrix on the order of 1000^3 voxels. However, the observed pressure sensitivity of the directly measured shear modulus might also include a contribution arising from finite compliance of the interfaces between the specimens and loading pistons – particularly for $P < 10$ MPa.

Dispersion and dissipation in the dry specimen

The elastic properties of the 'dry' reservoir sandstone specimen indicate a modest level of dispersion of both the Young's and shear moduli and associated strain-energy dissipation. For rocks under dry conditions, no (fluid-related) modulus dispersion and dissipation is expected. So such modest dispersion and dissipation for the nominally dry conditions are conceivably a manifestation of the presence of moisture in the pore spaces (e.g. Clark et al., 1980; Vigil et al., 1994; Pimienta et al., 2014; Yurikov et al., 2018) or frictional effects (e.g.Walsh,1966; Mavko, 1979). That moisture could be responsible for such observation is consistent with the findings of Vigil et al., (1994) on the nature of silica-water interfaces. They showed that a thin gel-like layer results from the effect of adhesion of moisture and frictional behaviour of the amorphous silica surface. Under those conditions, the frequency-dependence of the mechanical properties of porous material of predominantly quartz, especially with moisture on the siliceous surfaces at the intra-granular contacts, could be strongly favoured. For example, similar effects on nominally dry Navajo sandstone - initially vacuum-dried and then allowed to equilibrate for 28 days in 100% relative humidity air – documented by Spencer (1981) was interpreted as related to the presence of non-negligible moisture content.

There are possible sources of moisture in our reservoir sandstone specimen. We tested the specimen at the Curtin University 'as is' without any thorough drying protocol in an attempt to avoid undesirable

modification of the microstructure or the fluid-sensitive properties of the clay. So the remaining fluid (i.e. hydrocarbon and moisture) in this original sample may be described as "residual" from the fully saturated in-situ conditions. The strongest evidence of the influence of residual moisture is provided by comparing the 'dry' measurements of Young's modulus and ultrasonic compressional wave velocities, V_p measured at Curtin University and ENS. Both Young's modulus and ultrasonic V_p are substantially lower for the oven-dried than for the 'as-received' dry specimen, suggesting that the residual moisture stiffens the grain contacts. Effect of volatiles plausibly from the re-exposure to laboratory atmosphere during re-jacketing of the smaller-sized specimen tested at ANU could also partly be responsible for the non-negligible strain-energy dissipation observed in torsional oscillation under dry conditions (Fig. 5).

Frictional effects due to relative motions at the compliant inter-granular contacts (Mavko, 1979; Walsh, 1966) may also explain the observed Young's and shear dissipation for the dry reservoir sandstone specimen. Such frictional effect is consistent with the observation (in Figure 7) that the dissipation diminishes with increasing pressure and also likely contributed by interfacial compliance, particularly below 10 MPa.

4.2 Decane-saturated conditions

Fluid flow regimes and characteristic frequencies

It is well established that pore fluids strongly modify the mechanical properties of shallow crustal rocks to be frequency-dependent (Cleary, 1978; O'Connell & Budiansky, 1977). Such frequency-dependent behaviour can be described in terms of three fluid-flow regimes that are separated by transitions – each with a different relaxation mechanism. These transitions manifest as modulus dispersion and dissipation in the mechanical properties of fluid-saturated porous media (O'Connell & Budiansky, 1977).

At low-frequency conditions, pore fluid pressure perturbation within a homogenous porous medium has sufficient time to reach local equilibrium – meaning that any representative elementary volume of the porous medium has same pore fluid pressure and thus poroelastic theories apply. Such state of local equilibrium of pore pressure is referred to as the saturated isobaric (O'Connell & Budiansky, 1977). The

saturated isobaric regime is an undrained condition which is separated from the drained conditions at even lower frequencies by a transition characterised by a critical frequency given as (Cleary, 1978; Detournay & Cheng, 1993)

$$f_{\mathrm{dr}} = \frac{kK_f}{\Phi\eta l^2} \tag{6}$$

where k is the permeability of the medium, K_f is the bulk modulus of the pore-fluid, Φ is the porosity of the sample, η is the viscosity of the fluid, and l is the length scale over which pore fluid diffusion occurs, typically taken as between the half-and whole-length of the specimen.

At higher frequency, a critical frequency for squirt-flow f_{sq} describes the transition between saturated-isobaric and saturated-isolated fluid regimes. With K, α, η as the bulk modulus of the medium, crack aspect ratio and viscosity respectively, the squirt frequency (Jones, 1986; O'Connell & Budiansky, 1977) is given as

$$f_{\mathrm{sq}} = \frac{K\alpha^3}{2\pi\eta} \tag{7}$$

Using the data of Table 1, the characteristic length (80 mm) of the rock sample and aspect ratio, α of ~ 7 $\times 10^{-4}$, the draining and squirt frequencies for the decane-saturated conditions of the reservoir sandstone specimen are estimated as ~ 80 – 300 Hz and 2 kHz respectively.

Experimental boundary conditions

An important consideration in the comparison of inter-laboratory results on fluid-saturated porous media is the boundary condition imposed by the fluid drainage and control system on each experimental apparatus. The conditions of the fluid-saturated specimen are often assumed to be undrained. However, this is not always the case (Bishop, 1976; Ghabezloo & Sulem, 2010; Pimienta et al., 2015; Mikhaltsevitch et al., 2019). The nature and design of the pore pressure drainage and control system are essential. For example, Mikhaltsevitch et al. (2019) illustrated the effect of dead volume on the frequency

dependences of the elastic moduli of n-decane-saturated Savonnieres limestone specimens. In Pimienta et al., (2016) a one-dimensional poroelastic model was used to quantify the effect of boundary conditions imposed on a typical experiment with dead volume in the fluid drainage system at each end of the test specimen. Indeed, the dead volumes need to be taken into account in laboratory tests as it can strongly affect the measured dispersion and dissipation of a porous specimen because of its participation in the draining of the specimen. Rather than the measured dispersion and dissipation being genuinely related to the fluid within the pore network of the specimen, the measured properties also include the effect of possible fluid flow between the pore space of the specimen and the external pore-fluid reservoirs. Therefore the dead volume must be effectively zero or at least much smaller than the rock pore volume, to access the undrained conditions. So to compare and interpret the fluid flow regimes on the test reservoir sandstone specimen, it is critical to review the possible effect of the boundary conditions. Pore volumes of the specimen tested at ANU, and the other labs are ~ 4 cm^3 and 28 cm^3 respectively – reflecting the dimensional differences. For the test conducted at ENS, two drainage arrangements were used – one with 3.3 cm^3 (small) and the other with > 50 cm^3 (large) dead volume. For the test conducted at ANU and Curtin University, the dead volumes were 41.5 cm^3 and 2 cm^3 respectively. As all forced-oscillation tests were conducted at frequencies lower than f_{dr}, those involving the larger dead volumes will therefore probe drained conditions. Only the measurements with the lesser dead volumes of 2 cm^3 and 3.3 cm^3 at Curtin and ENS, respectively, could be expected to probe essentially undrained conditions for the reservoir sandstone specimen.

Accordingly, the stiffening by fluid saturation of the bulk modulus directly measured with oscillation of confining pressure must represent the (undrained) saturated isobaric regime - consistent with the expected effect of the presence of a relatively incompressible pore fluid such as decane, in the pore space. For such saturated-isobaric conditions, no fluid-related stiffening is expected for the shear modulus which is therefore expected to be the same as for drained conditions. However, given the sizeable dead volume relative to pore volume for the ANU apparatus as configured for this study, the forced torsional

oscillation tests at sub-Hz frequencies should have probed drained conditions with a shear modulus essentially unaffected by fluid saturation as observed. The possibility that the shear modulus might actually be reduced slightly by decane saturation at the lowest differential pressures (Fig. 5) might reflect lubrication of the inter-granular contacts. A much smaller dead volume of 1.5 cm^3, also available on the ANU apparatus, might be used to access undrained conditions in future measurements on highly permeable materials.

Reconciliation with the Gassmann model

The fact that the bulk modulus, whether directly measured at ENS or inferred from the axial-oscillation tests with small dead volume (Fig. 8), is systematically increased by decane saturation (Fig. 8), provides qualitative confirmation that the undrained regime was probed by these tests. Modelling the fluid-related stiffening of K and E for the saturated conditions allows an additional, more quantitative assessment. The well-known, low-frequency Gassmann equation (Gassmann, 1951) predicts the effects of pore fluids on the bulk and shear moduli of an isotropic homogenous medium within the saturated isobaric regime as follows

$$K_u = K_d + \Delta K; \tag{8}$$

$$\mu_u = \mu_d \tag{9}$$

where K_u is the undrained modulus, K_d the modulus of the dry rock frame, μ_d the shear modulus of the dry rock, μ_u the shear modulus of the saturated rock and ΔK is the increase in the bulk modulus due to fluid saturation of the dry rock, given as

$$\Delta K = \frac{\left(1-\frac{K_d}{K_m}\right)^2 K_f}{\phi+\left(\left(1-\frac{K_d}{K_m}\right)-\phi\right)\frac{K_f}{K_m}} \tag{10}$$

where K_m is the bulk modulus of the mineral matrix, K_f the bulk modulus of the pore fluid, K_d the bulk modulus of the dry rock medium, (drained of any pore-filling fluid), and ϕ the porosity. The observed

increase of bulk modulus upon decane saturation is well described by the Gassmann model with a bulk modulus of 33.1 GPa (Table 1) for the mineral skeleton (Fig. 8). This value is substantially less than that (37.6 GPa, McSkimin et al.,1965) for quartz alone, and hence is plausible for this impure sandstone (see e.g., Vernik, 1998). For a specimen with such a heterogeneous matrix (containing quartz and clay), the application of Gassmann's equation is not strictly rigorous. Indeed, the generalised equations of Brown & Korringa (1975) or Rice & Cleary, (1976) may be more appropriate. However, for shaly sandstones, the use of the standard Gassmann's equation is justified by the fact that clay is usually distributed uniformly. Modelling studies (e.g. in Zimmerman, 1991, page 59; Makarynska at al., 2007; Mavko & Mukerji, 2013) suggest that this approach is accurate unless rock heterogeneity is extreme.

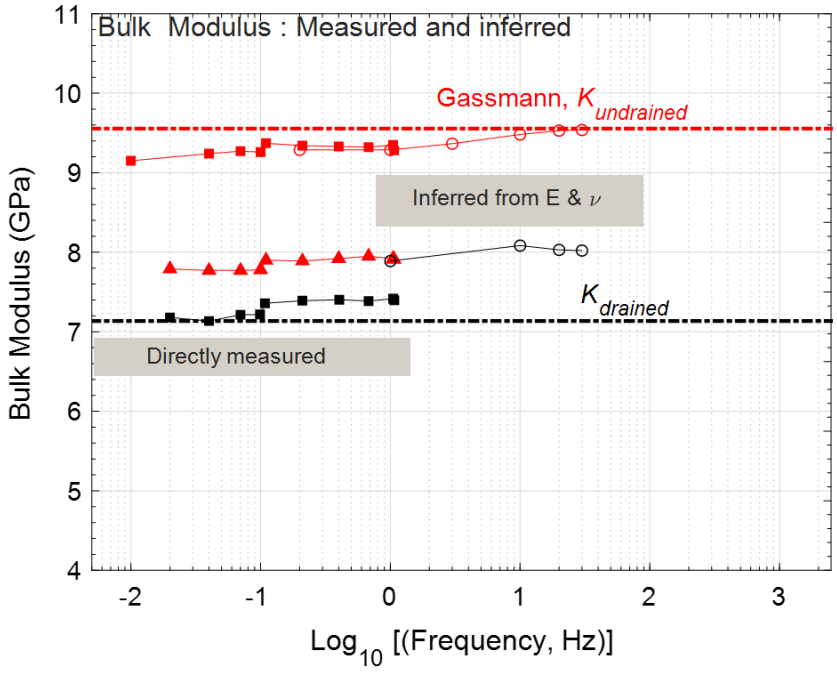

Figure 8: Frequency-dependence of the directly measured (square/triangle symbol = small/large dead volume) bulk modulus from confining pressure oscillation test (colours - red for sat and black for dry) compared with those inferred (in circles) by combining E and ν from axial forced-oscillation for measurements at Curtin University. Red broken line shows the Gassmann predictions. Differential pressure at 10 MPa.

The dry bulk modulus is ~ 7.1 GPa (as directly measured with the confining pressure oscillation test), the bulk modulus of decane pore fluid is 1.21 GPa (Table 1). The bulk modulus directly measured (at ENS) with small dead volume closely approaches the Gassmann's K_u. The fact that K directly measured with large dead volume is, reasonably, intermediate between K_d and K_u (Figure 8) suggests incomplete draining – highlighting the role of experimental boundary conditions. The fluid stiffening effect, represented by the spacing of the values of K inferred from axial stress oscillation tests dry and decane-saturated conditions with small dead volume is accurately predicted by the Gassmann model, but less so the absolute values of modulus at least for the ENS data.

The Gassmann value of K_u and the directly measured value of shear modulus $\mu = \mu_d = \mu_u$ can be combined ($E = 9K\mu/(3K+\mu)$ and $\nu = (3K - 2\mu)/(2(3K+\mu))$ to obtain E_u and ν_u respectively. We compared the obtained values of E_u and ν_u with the measurements in Fig. 4. Both the difference between values of E measured in the Curtin lab dry and decane-saturated, and the absolute values of the modulus are well described by the Gassmann model. For the ENS data, the same is true of the difference, but the absolute values are systematically lower. The Poisson's ratio for the fluid-saturated conditions, especially from results with the least dead volume (Curtin University), agrees quite well with Gassmann's ν_u. Therefore, it is reasonable to conclude that the elastic properties of the decane-saturated reservoir sandstone specimen are those of the undrained (saturated isobaric) conditions.

4.3 Broadband wave speeds

The broadband comparison in Fig. 9 indicates an only modest dispersion (2- 6 %) in P-wave velocity across the four decades of frequency separating the forced-oscillation and ultrasonic data (~ 2- 6 % relative to the ultrasonic value) - suggesting that the pressure dependence of wavespeeds or moduli from ultrasonic data would be broadly applicable at seismic frequencies.

For the S-wave velocities, however, the dispersion between the ultrasonic velocity and those inferred from the shear modulus directly measured at 0.01 Hz with the ANU apparatus is greater (~ 10-12 %).

Such dispersion is not unexpected given the pressure-dependent behaviour of both the shear modulus and ultrasonic velocity (Fig. 5 & 7) for the dry specimen, attributed to the closure of compliant inter-granular contacts. The presence of such compliant inter-granular contacts creates conditions favourable for squirt flow (with estimated characteristic frequency f_{sq} ~ 2 kHz) of the pore fluids between the inter-granular contacts and pores – possibly explaining the observed dispersion of the shear modulus but also contributing to dispersion of the bulk modulus.

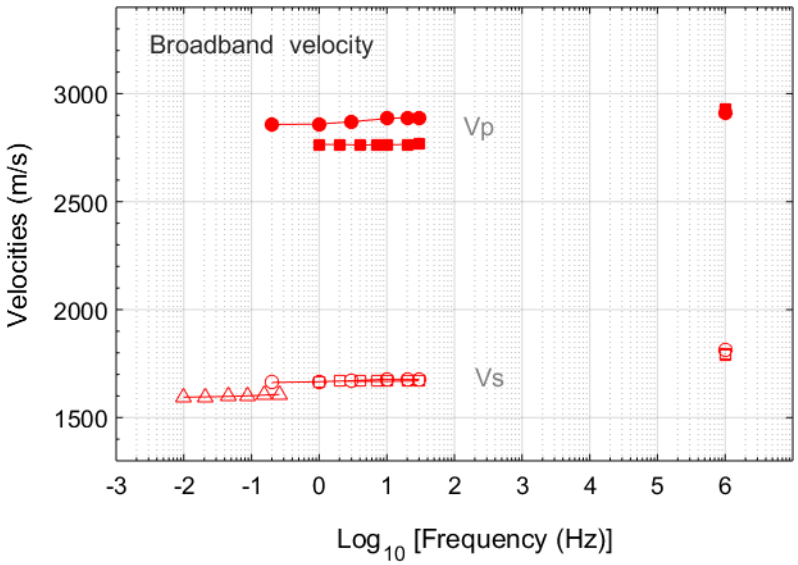

Figure 9: Broadband velocities for the decane-saturated specimen using results from axial oscillation, torsional oscillation and pulse transmission test, both at Curtin University (filled and open circle for *V*p and *V*s respectively) and ENS (filled and open square for *V*p and *V*s respectively) at 10 MPa differential pressure. *V*s inferred from ANU measurements in open triangles.

5.0 Conclusion

Systematic inter-laboratory testing of elastic properties of a fluid-saturated porous reservoir sandstone specimen has been conducted using complementary forced-oscillation and ultrasonic techniques in three different rock physics laboratories. Measurements have been made at seismic (0.01 to 40 Hz) and ultrasonic (1 MHz) frequencies of elastic moduli/velocities and Poisson's ratio at P_c = 10 MPa for the dry

specimen and P_d = 10 MPa for saturation with the n-decane. Young's modulus and Poisson's ratio were measured using axial forced-oscillation technique, shear modulus with torsional forced-oscillation and bulk modulus using oscillation of confining pressure.

The stiffening of the moduli (K and E) and Poisson's ratio observed on decane saturation of the specimen can be reconciled with the Gassmann model, suggesting that low-frequency testing with sufficiently small dead volume probes the undrained (saturated isobaric) conditions. Such fluid-related stiffening is more limited or absent for low-frequency measurements with dead volumes comparable with the pore volume of the specimen. Such measurements probe the systematically lower and frequency-dependent moduli associated with the transition towards drained conditions. Direct measurement of bulk modulus and shear modulus using approaches involving oscillation of confining pressure and the torsional forced-oscillation measurements, respectively, are consistent with those deduced from (E and ν, obtained) axial forced-oscillation measurements. We have attributed the pressure dependence of both the ultrasonic velocities and low-frequency shear modulus of the dry specimen to the progressive closure of compliant inter-granular contacts within the sandstone specimen. The presence of such compliant inter-granular contacts creates conditions favourable for squirt flow predicted at frequencies ~ 2 kHz, potentially responsible for the dispersion of shear and bulk moduli and compressional and shear velocity between forced-oscillation and ultrasonic frequencies.

Overall, the results of the inter-laboratory testing are consistent in terms of the effect of frequency and fluid saturation for the reservoir sandstone specimen. Such broad consistency illustrates the validity of forced-oscillation techniques and constitutes an important benchmarking study on elastic properties testing of a porous medium.

Data Availability Statement

The data supporting the findings in this paper belong to Woodside Energy Ltd and are not publicly available.

References

Adam, L., Batzle, M., & Brevik, I. (2006). Gassmann's fluid substitution and shear modulus variability in carbonates at laboratory seismic and ultrasonic frequencies. *Geophyscis*, *71*(6), F173-F183. Retrieved from https://doi.org/10.1190/1.2358494

Adam, L., Batzle, M., Lewallen, K. T., & Van Wijk, K. (2009). Seismic wave attenuation in carbonates. *J. Geophys. Res*, *114*. https://doi.org/10.1029/2008JB005890

Adelinet, M., Fortin, J., Guéguen, Y., Schubnel, A., & Geoffroy, L. (2010). Frequency and fluid effects on elastic properties of basalt: Experimental investigations. *Geophysical Research Letters*. https://doi.org/10.1029/2009GL041660

Asaka, M., Luo, M., Yamatani, T., Kato, A., Yoshimatsu, K., & Knapp, L. (2018). 4D seismic feasibility study: The importance of anisotropy and hysteresis. *Leading Edge*, *37*(9), 688–698. https://doi.org/10.1190/tle37090688.1

Batzle, M., Han, D., & Hofmann, R. (2006). Fluid mobility and frequency-dependent seismic velocity — Direct measurements. *Geophysics*, *71*(1), N1–N9. https://doi.org/10.1190/1.2159053

Birch, F. (1960). The velocity of compressional waves in rocks to 10 kilobars: 1. *Journal of Geophysical Research*, *65*(4), 1083–1102. https://doi.org/10.1029/JZ065i004p01083

Bishop, A. W. (1976). The influence of system compressibility on the observed pore-pressure response to an undrained in stress in saturated rock. *Geotechnique*, *26*(2), 371–375. https://doi.org/10.1680/geot.1976.26.2.371

Borgomano, J. V. M., Gallagher, A., Sun, C., & Fortin, J. (2020). An apparatus to measure elastic dispersion and attenuation using hydrostatic- And axial-stress oscillations under undrained conditions. *Review of Scientific Instruments*, *91*(3). https://doi.org/10.1063/1.5136329

Borgomano, J. V. M., Pimienta, L., Fortin, J., & Guéguen, Y. (2017). Dispersion and attenuation measurements of the elastic moduli of a dual-porosity limestone. *Journal of Geophysical Research: Solid Earth*. https://doi.org/10.1002/2016JB013816

Brown, R. J. S., & Korringa, J. (1975). on the Dependence of the Elastic Properties of a Porous Rock on the Compressibility of the Pore Fluid. *Geophysics*, *40*(4), 608–616. https://doi.org/10.1190/1.1440551

Cheng, C. H., & Toksöz, M. N. (1979). Pore Aspect Ratio Spectrum of a Rock. *Journal of Geophysical Research*, *84*(B13), 7533–7543.

Clark, V. A., Tittmann, B. R., & Spencer, T. W. (1980). Effect of volatiles on attenuation (Q^{-1}) and velocity in sedimentary rocks. *Journal of Geophysical Research*, *85*(B10), 5190. https://doi.org/10.1029/JB085iB10p05190

Cleary, M. P. (1978). Elastic and dynamic response regimes of fluid-impregnated solids with diverse microstructures. *International Journal of Solids and Structures*, *14*(10), 795–819. https://doi.org/10.1016/0020-7683(78)90072-0

Cline, C. J., & Jackson, I. (2016). Relaxation of the bulk modulus in partially molten dunite? *Geophysical Research Letters*, *43*(22), 11,644-11,651. https://doi.org/10.1002/2016GL071004

David, E. C., Fortin, J., Schubnel, A., Guéguen, Y., & Zimmerman, R. W. (2013). Laboratory measurements of low- and high-frequency elastic moduli in Fontainebleau sandstone. *Geophysics*,

78(5), D369–D379. https://doi.org/10.1190/geo2013-0070.1

Detournay, E., & Cheng, A. H. D. (1993). Fundamentals of poroelasticity. *Comprehensive Rock Engineering. Vol. 2, II*, 113–171. https://doi.org/10.1017/cbo9781139051132.003

Fortin, J., Schubnel, A., & Guéguen, Y. (2005). Elastic wave velocities and permeability evolution during compaction of Bleurswiller sandstone. *International Journal of Rock Mechanics and Mining Sciences*, *42*(7-8 SPEC. ISS.), 873–889. https://doi.org/10.1016/j.ijrmms.2005.05.002

Gassmann, F. (1951). Über die Elastizität poröser Medien. *Vier. Der Natur. Gesellschaft Zürich*, *96*, 1–23.

Ghabezloo, S., & Sulem, J. (2010). Effect of the volume of the drainage system on the measurement of undrained thermo-poro-elastic parameters. *International Journal of Rock Mechanics and Mining Sciences*, *47*(1), 60–68. https://doi.org/10.1016/j.ijrmms.2009.03.001

Gregory, A. R., & Podio, A. L. (1970). Dual-Mode Ultrasonic Apparatus for Measuring Compressional and Shear Wave Velocities of Rock Samples. *IEEE Transactions on Sonics and Ultrasonics*, *17*(2), 77–85. https://doi.org/10.1109/TSU.1970.7404096

Gurevich, B., Makarynska, D., Paula, O. B. De, & Pervukhina, M. (2010). A simple model for squirt-flow dispersion and attenuation in fluid-saturated granular rocks. *Geophysics*, *75*(6), N109–N120.

Han, D. H., Nur, A., & Morgan, D. (1987). The effects of porosity and clay content on wave velocities in sandstones. *Geophysics*, *51*(11), 2093–21007. https://doi.org/10.1190/1.1893163

Holt, R. M., Bauer, A., & Bakk, A. (2018). Stress-path-dependent velocities in shales: Impact on 4D seismic interpretation. *Geophysics*, *83*(6), MR353–MR367. https://doi.org/10.1190/geo2017-0652.1

Holt, R. M., Nes, O.-M., & Fjaer, E. (2005). In-situ stress dependence of wave velocities in reservoir. *The Leading Edge*.

Jack, I. (1997). *Time-Lapse Seismic in Reservoir Management*. *Time-Lapse Seismic in Reservoir Management* (SEG Distin). Society of Exploration Geophysicists. https://doi.org/10.1190/1.9781560802748

Jackson, I., & Paterson, M. S. (1993). A high-pressure, high-temperature apparatus for studies of seismic wave dispersion and attenuation. *Pure and Applied Geophysics*, *141*(2), 445–466. https://doi.org/10.1007/BF00998339

Jones, T. D. (1986). Pore fluids and frequency-dependent wave propagation in rocks. *Geophysics*, *51*(10), 1939–1953. https://doi.org/10.1190/1.1442050

King, M. S. (2009). Recent developments in seismic rock physics. *International Journal of Rock Mechanics and Mining Sciences*, *46*(8), 1341–1348. https://doi.org/10.1016/j.ijrmms.2009.04.008

Li, Y., David, E. C., Nakagawa, S., Kneafsey, T. J., Schmitt, D. R., & Jackson, I. (2018). A Broadband Laboratory Study of the Seismic Properties of Cracked and Fluid-Saturated Synthetic Glass Media. *Journal of Geophysical Research: Solid Earth*, 3501–3538. https://doi.org/10.1029/2017JB014671

Lu, C, & Jackson, I. (1996). Seismic-frequency laboratory measurements of shear mode viscoelasticity in crustal rocks I: competition between cracking and plastic flow in thermally cycled Carrara marble. *Physics of the Earth and Planetary Interiors*, *94*(1–2), 105–119. https://doi.org/10.1016/0031-9201(95)03079-4

Lu, Cao, & Jackson, I. (2006). Low-frequency seismic properties of thermally cracked and argon-saturated granite. *Geophysics*, *71*(6), F147–F159. https://doi.org/10.1190/1.2345053

Lumley, D. E., & Behrens, R. A. (1998). Practical Issues of 4D Seismic Reservoir Monitoring: What an Engineer Needs to Know. *SPE Reservoir Engineering (Society of Petroleum Engineers)*, *1*(6), 528–537.

Lumley, David E., Behrens, R. A., & Wang, Z. (1997). Assessing the technical risk of a 4D seismic project. In *1997 SEG Annual Meeting* (pp. 894–897). Society of Exploration Geophysicists. https://doi.org/10.1190/1.1437784

MacBeth, C. (2004). A classification for the pressure-sensitivity properties of a sandstone rock frame. *Geophysics*, *69*(2), 497–510. https://doi.org/10.1190/1.1707070

Makarynska, D., Gurevich, B., & Ciz, R. (2007). Finite Element Modelling of Gassmann Fluid Substitution of Heterogeneous Rocks. In *69th Annual International Conference and Exhibition, EAGE, Extended Abstracts, 2152*. European Association of Geoscientists & Engineers. https://doi.org/10.3997/2214-4609.201401645

Mavko, G. M. (1979). Frictional Attenuation : An Inherent Amplitude Dependence. *Journal of Geophysical Research*, *84*, 4769–4775.

Mavko, G. M., & Nur, A. (1979). Wave attenuation in partially saturated rocks. *Geophysics*, *2*(2), 161–178.

Mavko, G, & Mukerji, T. (2013). Estimating Brown-Korringa constants for fluid substitution in multimineralic rocks. *Geophysics*, *78*(3), L27–L35. https://doi.org/10.1190/GEO2012-0056.1

Mavko, G, Mukerji, T., & Dvorkin, J. (2009). *The Rock Physics Handbook: Tools for Seismic Analysis of Porous Media* (2nd ed.). Cambridge University Press. https://doi.org/10.1017/CBO9780511626753

Mavko, Gerald, & Nur, A. (1975). Melt squirt in the asthenosphere. *Journal of Geophysical Research*, *80*(11), 1444–1448. https://doi.org/10.1029/JB080i011p01444

McSkimin, H. J., Andreatch, P., & Thurston, R. N. (1965). Elastic moduli of quartz versus hydrostatic pressure at 25°and - 195.8°C. *Journal of Applied Physics*, *36*(5), 1624–1632. https://doi.org/10.1063/1.1703099

Mikhaltsevitch, V., Lebedev, M., & Gurevich, B. (2014). A laboratory study of low-frequency wave dispersion and attenuation in water-saturated sandstones. *Leading Edge*, *33*(6), 616–622. https://doi.org/10.1190/tle33060616.1

Mikhaltsevitch, V., Lebedev, M., Pervukhina, M., & Gurevich, B. (2019). A laboratory study of the effect of boundary conditions on the elastic moduli measurements. *81st EAGE Conference and Exhibition 2019*, *v*(June 2019). https://doi.org/10.3997/2214-4609.201900801

Müller, T. M., Gurevich, B., & Lebedev, M. (2010). Seismic wave attenuation and dispersion resulting from wave-induced flow in porous rocks — A review. *Geophysics*, *75*(5), 147–164. https://doi.org/10.1190/1.3463417

O'Connell, R. J., & Budiansky, B. (1977). Viscoelastic properties of fluid-saturated cracked solids. *Journal of Geophysical Research*, *82*(36), 5719–5735. https://doi.org/10.1029/JB082i036p05719

Ògúnsàmì, A., Borgomano, J. V. M., Fortin, J., & Jackson, I. (2020). Poroelastic Relaxation in Thermally Cracked and Fluid-Saturated Glass. In *Geophysical Research Abstracts, EGU General Assembly 2020*. https://doi.org/https://doi.org/10.5194/egusphere-egu2020-6001

Pimienta, L., Borgomano, J. V. M., Fortin, J., & Guéguen, Y. (2016). Modelling the drained/undrained transition: effect of the measuring method and the boundary conditions. *Geophysical Prospecting*,

64(4), 1098–1111. https://doi.org/10.1111/1365-2478.12390

Pimienta, L., Borgomano, J. V. M., Fortin, J., & Guéguen, Y. (2017). Elastic Dispersion and Attenuation in Fully Saturated Sandstones: Role of Mineral Content, Porosity, and Pressures. *Journal of Geophysical Research: Solid Earth*, *122*(12), 9950–9965. https://doi.org/10.1002/2017JB014645

Pimienta, L., Fortin, J., & Guéguen, Y. (2014). Investigation of elastic weakening in limestone and sandstone samples from moisture adsorption. *Geophysical Journal International*, *199*(1), 335–347. https://doi.org/10.1093/gji/ggu257

Pimienta, L., Fortin, J., & Guéguen, Y. (2015a). Bulk modulus dispersion and attenuation in sandstones. *Geophysics*, *80*(2), D111–D127. https://doi.org/10.1190/geo2014-0335.1

Pimienta, L., Fortin, J., & Guéguen, Y. (2015b). Bulk modulus dispersion and attenuation in sandstones. *Geophysics*, *80*(2), D111–D127. https://doi.org/10.1190/geo2014-0335.1

Rice, J. R., & Cleary, M. P. (1976). Some Basic Stress Diffusion Solutions for Fluid-Saturated Elastic Porous Media With Compressible Constituents. *Reviews of Geophysics and Space Physics*, *14*(2).

Sayers, C. M. (2005). Sensitivity of elastic-wave velocities to stress changes in sandstones. *Leading Edge (Tulsa, OK)*, *24*(12), 1262–1266. https://doi.org/10.1190/1.2149646

Sayers, C. M. (2006). Sensitivity of time-lapse seismic to reservoir stress path. *Geophysical Prospecting*. https://doi.org/10.1111/j.1365-2478.2006.00539.x

Siggins, A. F., & Dewhurst, D. N. (2003). Saturation, pore pressure and effective stress from sandstone acoustic properties. *Geophysical Research Letters*, *30*(2), 10–13. https://doi.org/10.1029/2002GL016143

Spencer, J. W. (1981). Stress Relations at Low Frequencies in Fluid Saturated Rocks: Attenuation and Modulus Dispersion. *Journal of Geophysical Research*, *86*(80), 1803–1812.

Spencer, James W. (1981). Stress Relaxations at Low Frequencies in Fluid-Saturated Rocks: Attenuation and Modulus Dispersion. *JOURNAL OF GEOPHYSICAL RESEARCH*, *86*(10), 1803–1812. https://doi.org/10.1029/JB086iB03p01803

Subramaniyan, S., Quintal, B., Tisato, N., Saenger, E. H., & Madonna, C. (2014). An overview of laboratory apparatuses to measure seismic attenuation in reservoir rocks. *Geophysical Prospecting*, *62*(6), 1211–1223. https://doi.org/10.1111/1365-2478.12171

Vernik, L. (1998). Acoustic velocity and porosity systematics in siliciclastics. *Log Analyst*, *39*(4), 27–35.

Vigil, G.; Xu, Z. H.; Steinberg, S.; Israelachvili, J. (1994). Interactions of Silica surfaces. *J. Colloid Interface Sci.*, *165*(2), 367–385.

Vigil, G., Xu, Z. H., Steinberg, S., Israelachvili, J., & Washburn, E. W. (1994). Interactions of Silica surfaces. *J. Colloid Interface Sci.*, *165*(2), 273–283. https://doi.org/10.1103/PhysRev.17.273

Walsh, J. B. (1965). The effect of cracks on the uniaxial elastic compression of rocks. *Journal of Geophysical Research*, *70*(2), 381–389. https://doi.org/10.1029/JZ070i002p00381

Walsh, J. B. (1966). Seismic wave attenuation in rock due to friction. *Journal of Geophysical Research*, *71*(10), 2591–2599. https://doi.org/10.1029/jz071i010p02591

Wang, Z. (1997). Feasibility of time-lapse seismic reservoir monitoring: The physical basis. *The Leading Edge*, *16*(9), 12090–1360.

Yurikov, A., Lebedev, M., Gor, G. Y., & Gurevich, B. (2018). Sorption-Induced Deformation and Elastic Weakening of Bentheim Sandstone. *Journal of Geophysical Research: Solid Earth*, *123*(10), 8589–8601. https://doi.org/10.1029/2018JB016003

Zimmerman, R. W. (1991). *Compressibility of sandstones*. Amsterdam;New York:New York,NY,USA: Amsterdam ; New York : New York, NY, USA. Elsevier;Distributors for the United States and Canada, Elsevier Science Pub. Co.